Erez Halahmi,[1] M.Sc.; Ofra Levi,[2] M.Sc.; Leeor Kronik,[3] Ph.D.; and Raymond L. Boxman,[4] Ph.D.

Development of Latent Fingerprints Using a Corona Discharge

REFERENCE: Halahmi E, Levi O, Kronik L, Boxman RL. Development of latent fingerprints using a corona discharge. J Forensic Sci 1997;42(5):833–841.

ABSTRACT: A novel technique for the development of latent fingerprints is presented. It is based on placing a fingerprint-bearing object inside a corona discharge induced plasma. The development of various real and artificial fingerprints on metallic substrates under a wide range of conditions is studied. Using the results of the development experiments and the results of X-ray photoelectron spectroscopy, it is shown that the development is based on oxidation of the fingerprint background. This is achieved by strong oxidizers generated by the discharge process, while saturated fatty-acids found in sebaceous fingerprints protect the area beneath them, resulting in a visible fingerprint. The process is optimized by minimizing the electrode gap distance and maximizing the peak discharge voltage and the pulse repetition frequency.

KEYWORDS: forensic science, criminalistics, latent fingerprints, metal surfaces, corona discharge-induced-plasma

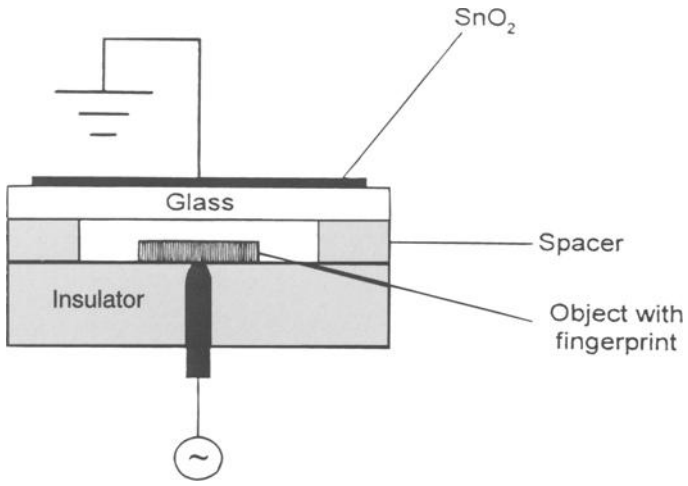

FIG. 1—*Experimental setup for the development of latent fingerprint using a corona discharge.*

Analysis of human fingerprint ridge patterns is a ubiquitous method for associating a criminal with evidence found in a crime scene. Unfortunately, many of the fingerprints found are latent, i.e., they are invisible to the naked eye. Therefore, great efforts for their visualization are made by forensic science laboratories around the world almost every day, using a variety of techniques (1). Hence, any new method for the detection of latent fingerprints is of interest, as it may find certain applications where no other technique is more effective or less expensive. One such novel method is presented in this paper. The new technique is based on placing the fingerprint-bearing object inside a corona discharge-induced-plasma (2). A corona discharge is a partial electrical discharge which is characterized by a high voltage (several kV), and a low current (a few mA) (2).

Experimental

As mentioned above, the proposed technique consists of placing an object inside a corona discharge-induced plasma. The setup used to generate the corona discharge is shown in Fig. 1. The object is placed on a (bottom) hemispherical metallic electrode with a 3-mm diameter. A 2-mm thick glass plate coated with a film of SnO_2 (a transparent conductor) on the top side (3), is used as a top electrode with an attached insulating dielectric material. Two glass plates, the thickness of which is adjusted to yield an air gap of 1.5 mm, are used as spacers. An air gap is left between the top electrode and the object. Latent fingerprints were obtained as follows: For sebaceous fingerprints, a clean finger was brushed across the forehead just before fingerprint deposition. For eccrine fingerprints, a clean finger was placed in a clean plastic glove for approximately 10 min prior to fingerprint deposition. In order to develop a latent fingerprint on an object, the latter is placed on the lower electrode. High voltage pulses are then applied to the electrode, producing a corona discharge between the object and the upper electrode. Unless otherwise noted, all the development experiments described below were conducted using this setup. All objects used were cleaned prior to fingerprint deposition with a commercial metal cleaning material ("Silvo Duraglit", Reckitt and Colman, Spain), rinsed, and dried. The latent fingerprints become visible within a few seconds to a few minutes of voltage application, depending on the discharge parameters. In the experiments described below, (unless otherwise noted) a train of pulses with a total duration of 140 s, composed of alternating 16 s long pulse bursts and 4 s of no bias (in order for the glass electrode to cool down), was used. Each pulse burst was composed of 17.5 kV, 340 μS (full width half maximum) pulses at a repetition rate of 500 Hz, producing a maximal current of 100 mA.

For some experiments used to elucidate the development mechanism, the setup shown in Fig. 2 was used. In this setup, the upper electrode is placed diagonally, and thus the distance between the electrodes gradually increases. Because within the spacing range of the first setup, the probability of discharge occurrence decreases with increasing electrode spacing (2), the discharge will take place

[1]Formerly student, Electrical Discharge and Plasma Laboratory and Department of Interdisciplinary Studies, Faculty of Engineering, Tel-Aviv University, Ramat-Aviv 69978, Israel.

[2]Ph.D. student, Department of Chemistry, Technion—Israel Institute of Technology, Technion City, Haifa 32000, Israel.

[3]Research associate, Department of Physical Electronics, Faculty of Engineering, Tel-Aviv University, Ramat-Aviv 69978, Israel.

[4]Director, Electrical Discharge and Plasma Laboratory and Professor of Electrical and Electronics Engineering, Tel-Aviv University, Ramat-Aviv 69978, Israel.

Received 15 July 1996; and in revised form 2 Dec. 1996; accepted 3 Dec. 1996.

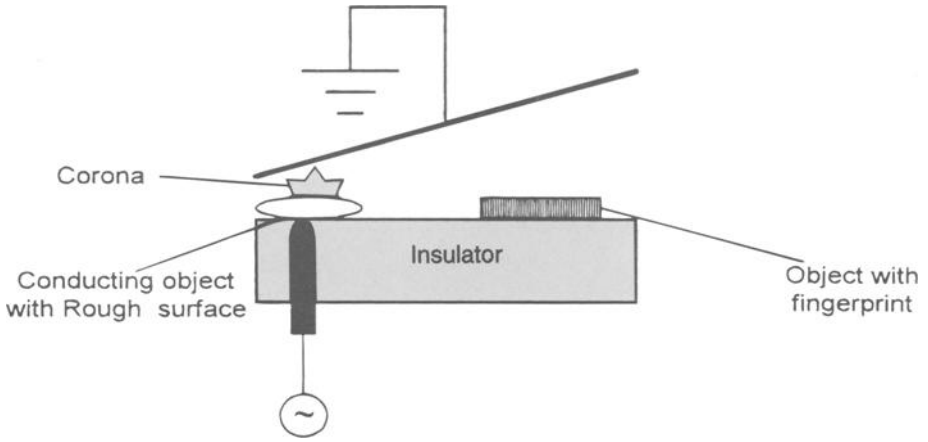

FIG. 2—*Alternative experimental setup for the development of latent fingerprint using a corona discharge in which the object is outside of the discharge region.*

only where the top electrode is close enough to the bottom one. Thus, if the object under investigation is placed where the inter-electrode distance is large (and on an insulator), it is *not* a part of the discharge process. Hence, the electrical discharge has no *direct* influence on the object. However, the discharge-generated plasma may still affect the object by diffusion. To that end, the overall plasma generation rate was enhanced by replacing the lower electrode of the first setup with a conducting rough surface (typically, a coin). The rough surface has a multitude of sharp points at which the electric field is enhanced. Thus, the number of micro-discharges per unit area, and hence plasma generation are enhanced.

Results

Figures 3a and 3b feature a $^1/_2$ shekel coin on which a sebaceous fingerprint has been deposited, before and after development, respectively. Note that before the development the fingerprint is barely visible. No clear, if any, characteristic points are observed. However, a clear fingerprint is revealed after development. The resulting fingerprint contains many characteristic points so that a comparison of it with other fingerprints (e.g., with fingerprints taken from a data base) is made possible. The resulting image is "negative" with respect to an inked fingerprint, i.e., it consists of bright ridges on a darker background.

In this section, experiments designed to shed light on the physical/chemical mechanisms responsible for results such as those shown in Fig. 3 are presented. A detailed discussion and interpretation of them is presented in the next section.

Clearly, it is very important to isolate the fingerprint components which actually contribute to the development process. To that end, the following sweat ingredients were tested: 1-alanin, 1-isoleucine, glycine, 1-phenylalanine, 1-lactic acid, trioleic-glycerid, palmitic acid, and stearic acid. This is a representative set of the organic components in a human fingerprint (4). Each of the above mentioned materials was dissolved in extra dry (spectral) benzene with a ratio by weight of 99.9% benzene to 0.1% of the tested material (4). Each of the resulting eight solutions is referred to henceforth as "artificial sweat". Assuming the reaction of each fingerprint component with the corona-induced plasma is independent of the reaction of the other ones, any "fingerprint" made using "artificial sweat" serves to determine whether the corresponding sweat component contributes to the development of the fingerprint. This is achieved by observing whether the latent fingerprint becomes visible or not.

Each type of "artificial sweat" (as well as a control sample with benzene only) was deposited on a brass plate using a rubber stamp in the form of parallel strips and subjected to the corona-discharge process described in the preceding section. The distance between the parallel strips decreases from ~0.6 mm at the edges towards ~0.05 mm at the center. Only "fingerprints" prepared using palmitic and stearic acids could be clearly observed after the development process. A typical developed "artificial fingerprint" (based on palmitic acid) is shown in Fig. 4. (A control sebaceous fingerprint is deposited on the left corner of the "artificial fingerprint".) The resultant image is similar to the one shown in Fig. 3b. Again, in both cases the image is in a "negative" form. All parallel strips were resolved after development.

Another set of similar experiments was conducted using real human fingerprints. A sebaceous fingerprint was always visible after development, even if the fingerprint-bearing brass plate was put in water for 24 h prior to development. However, eccrine fingerprints were not visible after development with or without a similar water treatment.

An additional experiment was concerned with the response of the development method to saturated fatty acids versus unsaturated fatty acids. Spots of trioleic-glycerid-based and stearic-acid-based (unsaturated and saturated fatty acids, respectively) "artificial sweat" were dripped on a clean copper plate. The results after development are shown in Fig. 5. The stearic-acid-based drop is clearly visible, whereas the trioleic-glycerid-based drop is barely visible.

In order to check whether the discharge process has any direct influence on the development procedure, the experimental setup shown in Fig. 2 was also used to develop both real (sebaceous) and "artificial" (palmitic and stearic acids) fingerprints. The object was placed at a distance of 4 cm from the rough surfaced-electrode on an insulator. During the discharge, no light was visible from the sample area, i.e., no discharge-related visible streamers or feathers (2) began or ended near the object, indicating that it indeed took no part in the discharge process. Applying the same voltage as before, all fingerprints were visible after development as in the previous setup.

Another set of experiments was concerned with attempting to

FIG. 3a

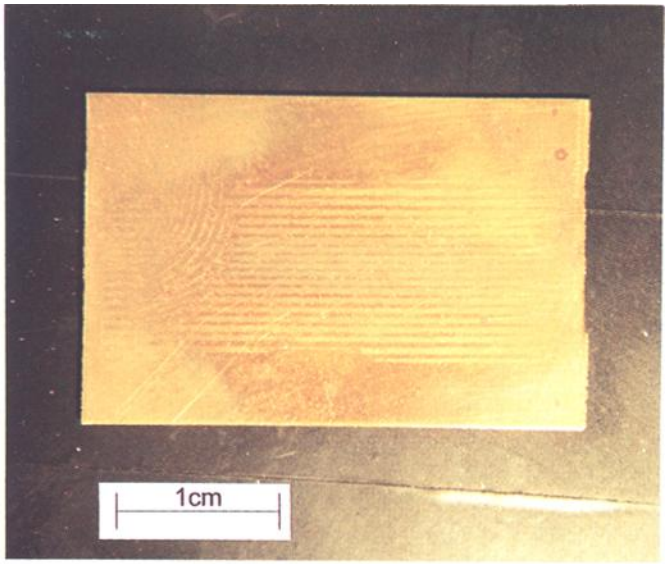

FIG. 4

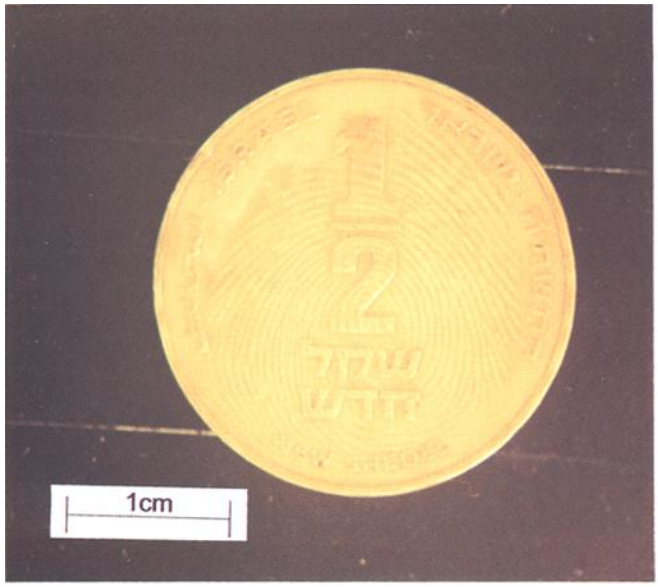

FIG. 3b

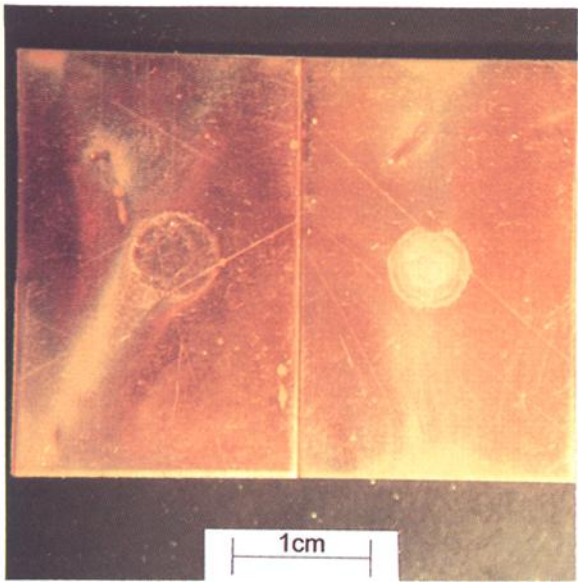

FIG. 5

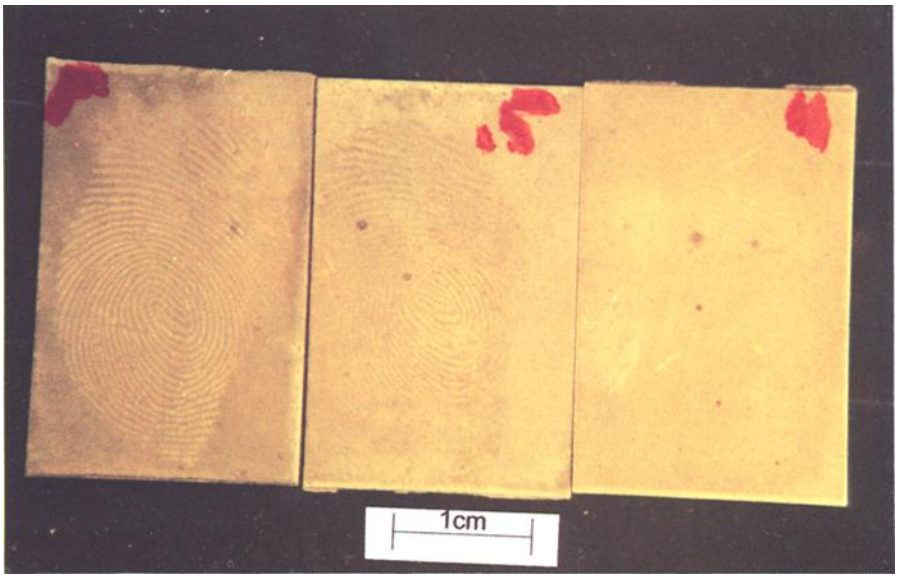

FIG. 6

See overleaf for captions.

optimize the operating characteristics of the corona discharge, so as to obtain the best development results possible (i.e., maximum contrast). Specifically, the desired height of the inter-electrode air gap and the electrical pulse amplitude and frequency were studied. The results of air gap optimization experiments are shown in Fig. 6, which features the results of the development of sebaceous fingerprints for three different air gaps: 4 mm, 0.5 mm, and less than 20 μm. It is easily seen that indeed the smaller the air gap, the better the results. The corona images photographed during the development process for the different air gaps of Fig. 6 are shown in Fig. 7. The images were obtained by positioning a regular 35 mm camera *outside* the active media, above the glass electrode (5). (Additional parameters—lens focal length: 80 mm, F#: 5.6, film ASA: 200 (Kodak), exposure time: 20 s). Using the figure, it is readily observed that the 4-mm air gap is too large to enable a discharge from the plate surface, which explains the poor results of the development. In the case of the other two air gaps, a discharge between the entire plate surface and the glass electrode occurred during development. Similar experiments concerned with the optimization of pulse amplitude and frequency have also been conducted. It was found that a pulse amplitude of 17.5 kV yielded better results than a 16 kV amplitude, and that a pulse frequency of 500 Hz yielded better results than a 50 Hz frequency. It is worthwhile to note that the development procedure is not very sensitive to the optimization parameters studied, so that similar results are obtained over a wide range of parameters.

X-ray photoelectron spectroscopy (XPS) (6) was used to investigate the physical/chemical processes causing the fingerprint development. In XPS, the energy distribution of electrons emitted from the sample due to irradiation with X-ray photons is studied. This distribution indicates the species present at the sample surface as well as their chemical state. XPS data were taken for two copper samples. One half of each sample was covered with palmitic-acid-based "artificial sweat" whereas the other half remained unaltered. One sample was measured as is while the other was measured after development. Both samples were cleaned prior to "artificial sweat" deposition and XPS measurements using a standard ultra-high vacuum procedure consisting of the following steps: 1. Water and soap rinse. 2. Pure water rinse. 3. Acetone rinse in an ultrasonic bath for 10 min. 4. Same as step 3, only with ethanol. 5. Cleaning with "Silvo Duraglit". 6. repeat of steps 2-4. All XPS measurements were conducted using a PHI 5600 multi-technique system (Physical Electronics Industries, USA). An Al Kα X-ray

See preceding page for figures 3 to 6.

FIG. 3—*Sebaceous fingerprints deposited on a $^1/_2$ shekel coin: (a) before treatment, (b) after development with a corona discharge.*

FIG. 4—*Palmitic-acid-based "artificial sweat" deposited on a brass plate, after development (A control sebaceous fingerprint is deposited on the left corner).*

FIG. 5—*Drops of stearic acid (right plate) and trioleic-glycerid (left plate) deposited on copper, after development.*

FIG. 6—*Developed sebaceous fingerprints on brass plate with an air gap of 4 mm (right plate), 0.5 mm (middle plate), and less than 20 μm (left plate).*

FIG. 7—*Corona images taken during the development of the fingerprints presented in Fig. 6: (a) 4-mm air gap, (b) 0.5-mm air gap, and (c) less than 20-μm air gap.*

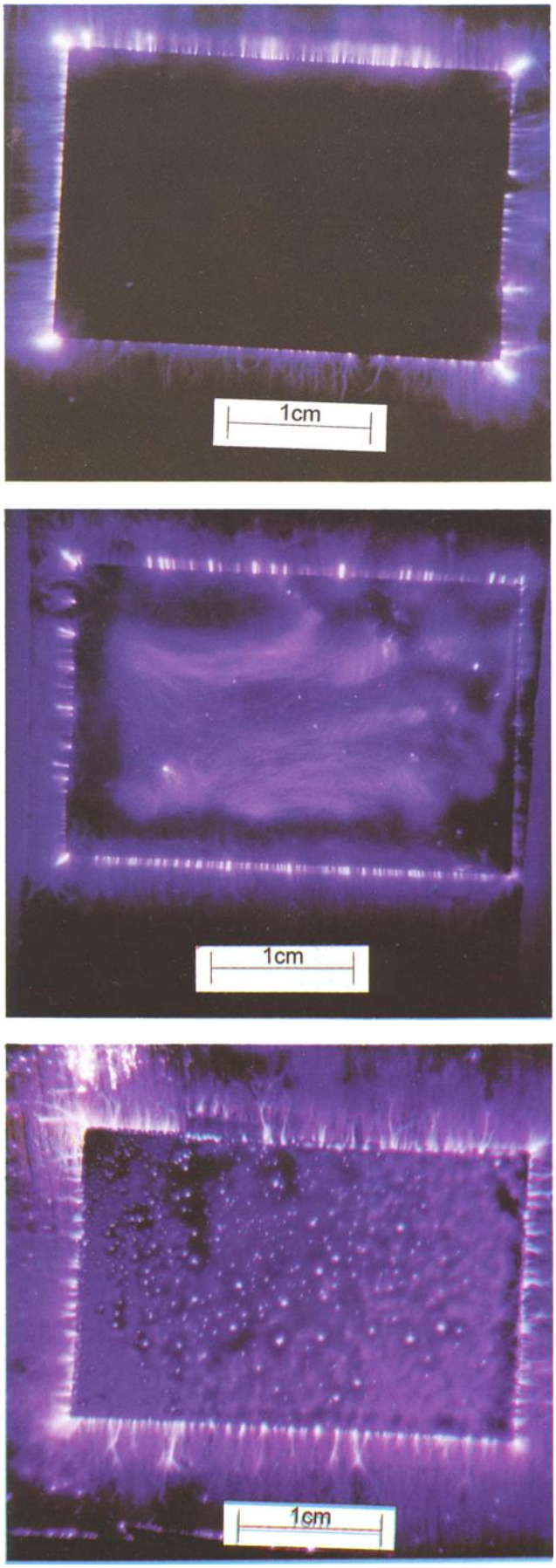

FIG. 7

source (1486.6 eV) provided the incident radiation. The spot size was 400 μm and the pass energy was 2.950 eV. In the depth-profiling experiments given below, 4 keV Ar^+ ions were used (their sputtering rate for SiO_2 on Si is 10Å/min).

Figures 8, 9, and 10 feature the X-ray photoelectron spectra taken from the two samples in the range of the Cu 2p peaks. In Fig. 8, the spectra before and after development are compared for the uncovered areas (a) and the covered areas (b). Similarly, in Fig. 9 the spectra of covered and uncovered areas are compared before (a) and after (b) development. In addition, the atomic concentrations of copper and oxygen in the different samples and regions are given in Table 1. The results of a depth profiling experiment of the developed areas are shown in Fig. 10 for the uncovered (a) and the covered (b) areas.

The findings of the XPS experiments may be summarized as follows: The XPS peaks at 932.6 eV and 952.9 eV, together with a peak at 567.5 eV (not shown) which corresponds to the Cu LMM transition (kinetic energy: 918.6 eV), correspond to emission from (unoxidized) Cu (7). Therefore, it is clearly seen that before development the copper plate is unoxidized whether it is covered or not. The appearance of *additional* peaks at 942.5 eV and 962.4 eV corresponds to emission from Cu oxidized to the second degree (7). Thus, after development, oxidized copper appears in the spectra of both covered and uncovered areas. However, the extent of oxidation is much larger in the uncovered sample, as judged by the relative height of the additional XPS peaks. Moreover, after 15 min of sputtering, the signal corresponding to oxidized copper is larger in the spectrum of the uncovered area. In contrast, it has completely disappeared from the spectrum of the covered area, whereas the signal corresponding to unoxidized copper has increased. After 45 min of sputtering, oxidized Cu is not seen in either sample.

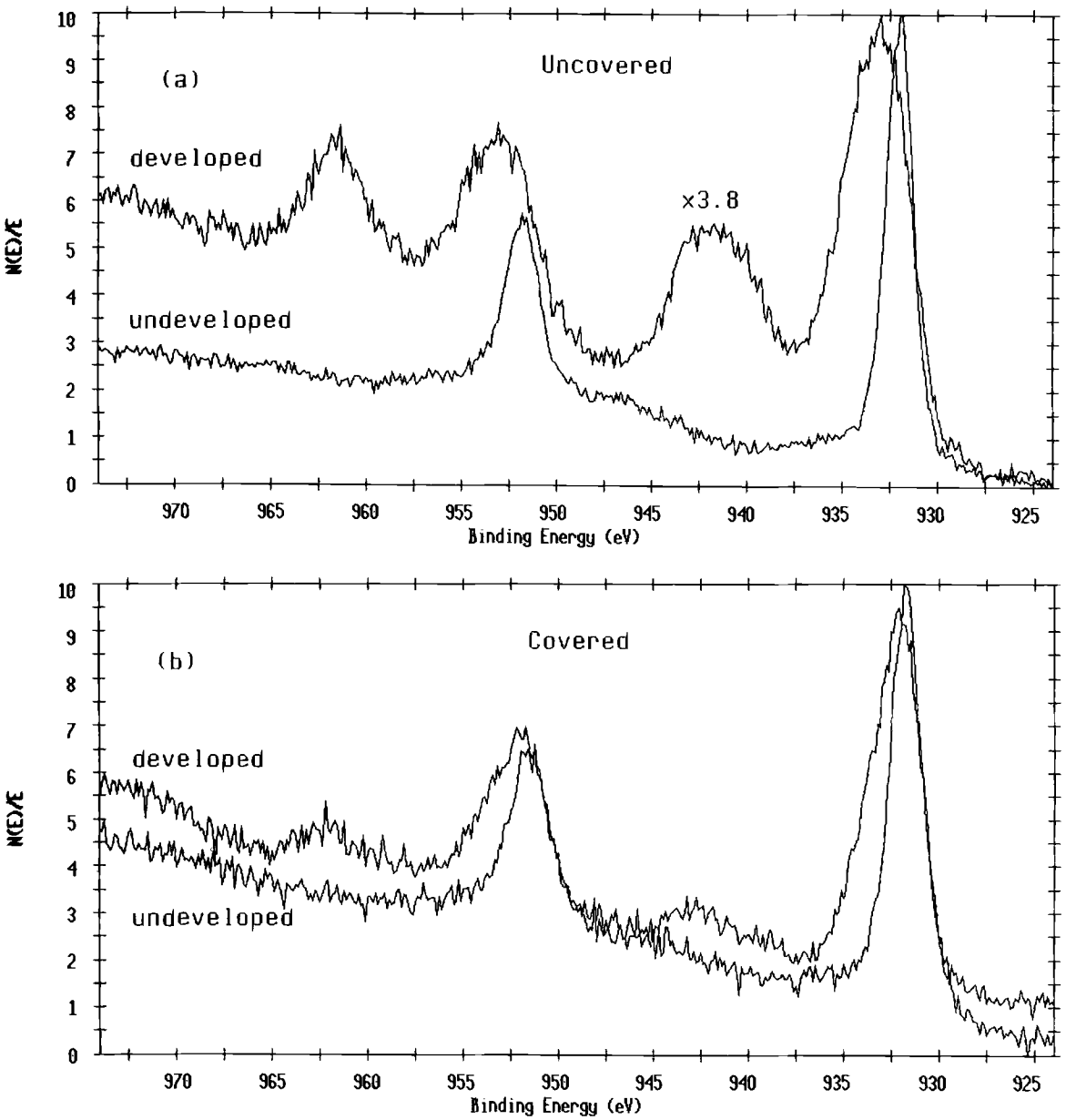

FIG. 8—*X-ray photoelectron spectra taken before and after development from an uncovered (a) and covered with palmitic acid, (b) copper plate in the vicinity of the Cu 2p peak.*

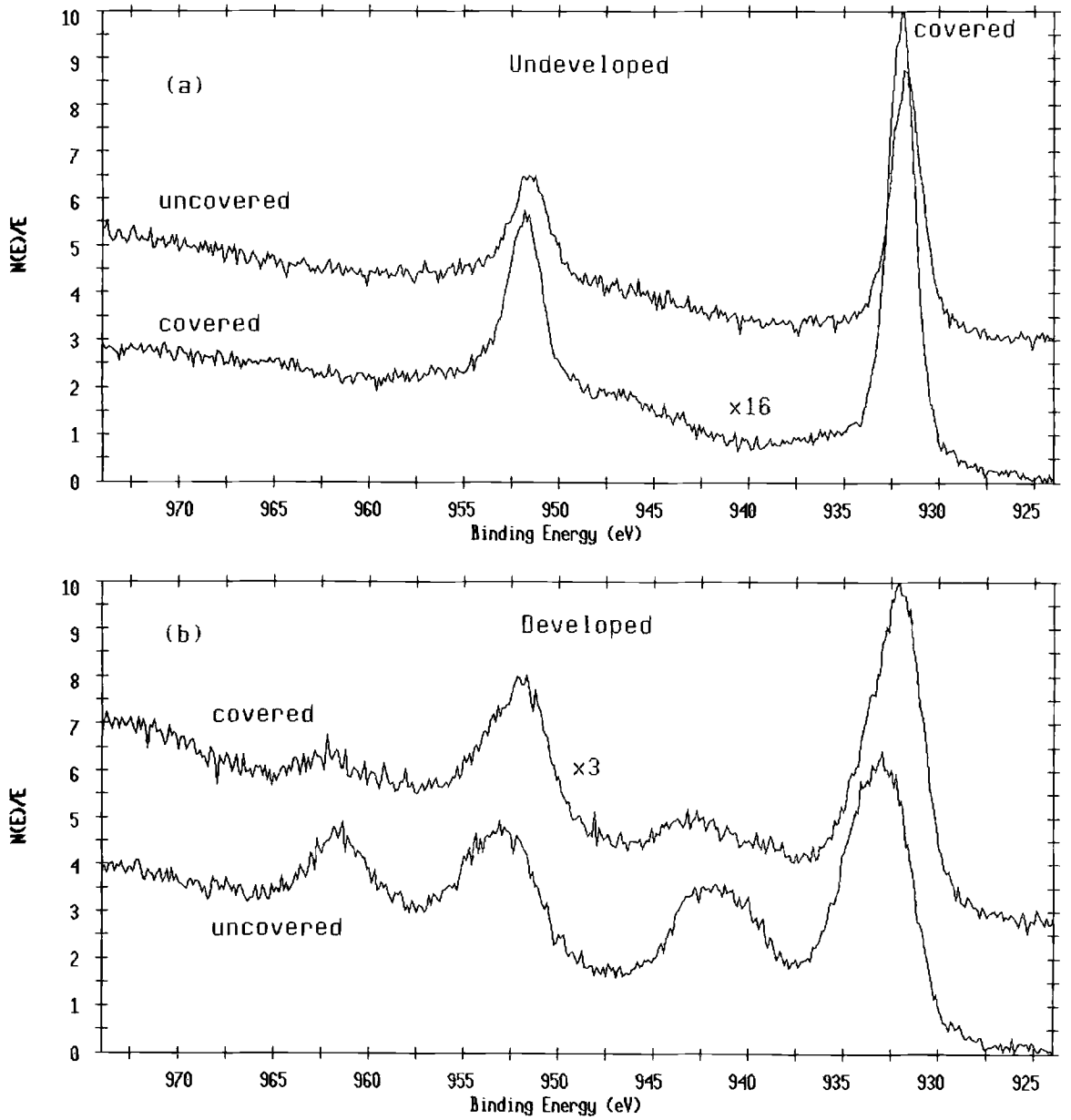

FIG. 9—*X-ray photoelectron spectra taken from an area covered with palmitic acid, and uncovered area of an undeveloped. (a) and developed, (b) copper plate in the vicinity of the Cu 2p peak.*

Using Table 1, we note that some copper signal is visible even in the covered areas even before sputtering. Furthermore, we observe that the atomic percent of oxygen increases after development. This increase is much larger in the uncovered region than in the covered region. Thus, we conclude that: (a) The development procedure oxidizes the copper. (b) Covering the sample with palmitic-acid-based "artificial sweat" greatly reduces the extent of the oxidation as well as its penetration depth.

Discussion

Based on the results of the experiments presented in the preceding section, it is possible to construct a mechanism for the corona development phenomena. In this section, we present the mechanism and show how it explains all the experimental observations given above. The suggested mechanism is as follows: The development of the fingerprints is a chemical process. The corona discharge process in air generates ozone and other oxidizing species, e.g., atomic oxygen (8). These species are strong oxidizers, far more chemically active than O_2 molecules, and easily oxidize the substrate on which the fingerprint is deposited. However, the material deposited from the fingerprint ridges may protect the substrate from oxidation. In particular, the saturated fatty acids present in sebaceous fingerprints provide such protection. Then, if the substrate changes color upon oxidation, the change in color between the oxidized areas (fingerprint valleys) and the protected areas (fingerprint ridges) results in a "developed" fingerprint which is visible to the naked eye. Specifically, the copper substrate darkens upon oxidation, resulting in a "negative" image, as mentioned above. It is important to note that while the experiments given

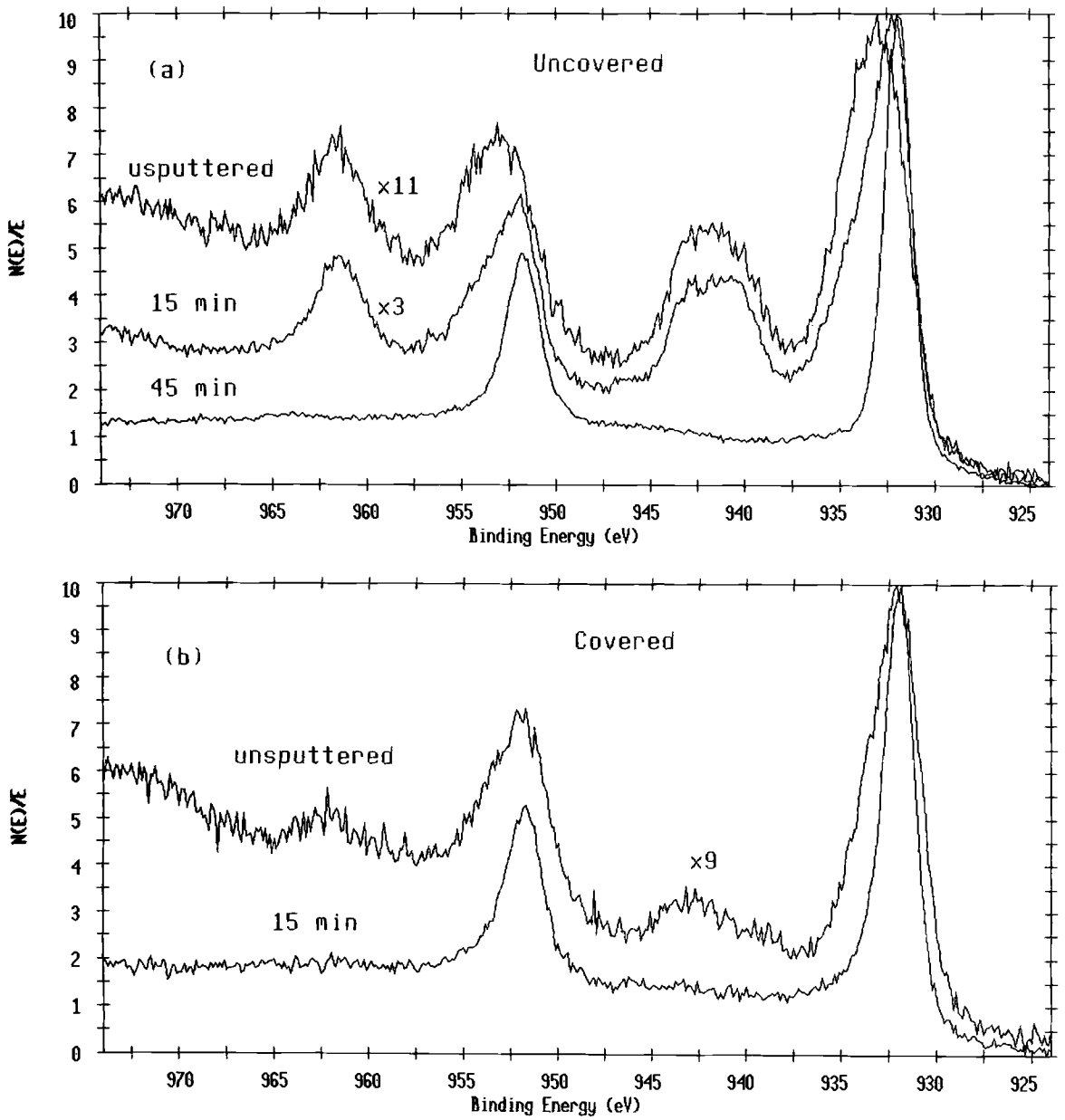

FIG. 10—*X-ray photoelectron spectra taken from an uncovered: (a) and covered with palmitic acid, (b) copper plate in the vicinity of the Cu 2p peak, for several sputtering times, after development.*

here have been performed on metallic substrates, non-metallic objects undergo the same physical and chemical processes under the above presented development conditions. Thus, the same development mechanism is expected to apply for any substrate which changes color upon oxidation, whether metallic or not.

TABLE 1—*Atomic concentration of Copper and Oxygen on a free or covered with Palmitic-acid based "artificial sweat" Copper surface, before and after development.*

	Undeveloped Sample		Developed Sample	
Element	covered (%)	uncovered (%)	covered (%)	uncovered (%)
Copper	2.8	29.1	4.5	21.1
Oxygen	13.7	14.3	19.4	40.2

The chemical nature of the observed phenomena is made clear by the results of fingerprint development with the setup shown in Fig. 2. As explained in the preceding section, in this setup the sample takes no part in the discharge process. Nevertheless, the results of all fingerprint developments were similar to those obtained using the setup shown in Fig. 1. Thus, it is quite obvious that the various physical processes involved in the corona discharge (e.g., electron and ion bombardment) are of no consequence to fingerprint development. This is consistent with the proposed mechanism because the generated oxidizing species reach the sample of the apparatus shown in Fig. 2.

The main body of evidence in support of substrate protection and/or oxidation is provided by the results of the XPS measurements: The underlying copper (i.e., the substrate) is initially unoxidized, and remains so after being covered by the "artificial sweat". Following the development, the bare substrate is greatly oxidized.

However, the "artificial sweat" covered substrate (equivalent to the region under the fingerprint ridges) is only lightly oxidized, both in terms of the oxidized-copper-related XPS signal (see Fig. 8 and Fig. 9) and in terms of the depth of the oxidized region (see Fig. 10). We believe the light oxidation found is due to pores in the covering material. Such pores are also to be expected in real fingerprints. This conclusion is corroborated by the presence of some copper-related signal in the (surface sensitive) X-ray photoelectron spectrum of the covered area both before and after development (see Table 1).

The protection of the substrate from oxidation by saturated fatty acids is made clear by the results of the development experiments with different sweat ingredients and "artificial sweats". All fingerprint development attempts with sweat ingredients composed of relatively short molecules, e.g., amino acids, failed. This indicates that such materials do not provide good protection against substrate oxidation. Accordingly, only non-water-soluble fingerprint components could be observed using our technique, because all water-soluble ingredients are composed of relatively short molecules. Since the great majority of eccrine gland constituents are water soluble, it is easy to understand why development of eccrine fingerprints failed. Thus, it is mainly the non-water-soluble ingredients of fingerprints which are involved in the development process. Sebaceous fingerprints include a small amount of water-soluble components, which may react as well during development. Hence, some influence of water-soluble compounds, although unlikely, cannot be completely ruled out.

It is interesting to note that ozone is known to attack double bonds existing in unsaturated fatty acids (9) (e.g., trioleic-glycerid) and thus split such acids into smaller molecules. As explained above, shorter chains provide less protection against oxidation. Hence, our proposed mechanism also explains why the drop based on a saturated fatty acid (stearic) shown in Fig. 5 is clearly visible, whereas the drop based on unsaturated fatty acid (trioleic-glycerid) shown in the same figure is barely visible.

Because we have satisfactorily explained all experimental results using a chemical oxidation model, one may ask why use an electrical discharge at all instead of an alternative ozone (or other oxidizing species) source. In practice, however, the only commercial method for ozone generation is an electrical discharge (9,10). After its generation, the ozone decomposes rapidly and therefore cannot be stored well, unless a complicated procedure is performed (9). Moreover, ozone is highly explosive (11). Similar observations hold for other oxidizing species generated by the electrical discharge.

Because the model presented above explains the development process in terms of exposure to ozone and other highly active oxidizing species, it predicts that the development would be optimal when the conditions for generating these species are optimal. It has been shown (10) that the optimal conditions for such generation in air are a minimal air gap and maximal pulse amplitude and frequency, within the following restrictions: a. The pulse period must not exceed the micro-discharge duration (10) (i.e., the minimal possible time between two consecutive streamers emanating from the same point, typically ~1–10 ns). b. The air gap must be large enough to enable the occurrence of a discharge, as given by the Paschen relation (2). Hence, the optimal air gap is slightly larger than the Paschen minimum, and is of the order of a few microns under atmospheric pressure. c. The pulse amplitude must be below damage threshold (to the electrode or to any material within the plasma). By considering the optimization results presented in the results section, it becomes clear that the predictions of the above presented model are confirmed experimentally. Indeed, the development improves with decreasing inter-electrode spacing and increasing pulse amplitude and frequency. The optimization results discussed here serve two purposes. On the one hand, they indicate how to obtain better developed fingerprints. On the other hand, they serve to corroborate the proposed model further.

Conclusions

A novel technique has been presented for the development of latent fingerprints, based on placing the sample in an oxidizing environment induced by a corona discharge. It has been shown to be useful for non-porous objects with sebaceous fingerprints, whether they have a smooth or a rough surface and whether they are wet or dry objects. A development mechanism is proposed based on production of oxidizing species, such as ozone, in the corona discharge and subsequent oxidation of the fingerprint background (substrate), while saturated fatty acids present in the fingerprint protect the substrate underlying it from oxidation. This leads to a "negative" visible image. A minimal air gap and maximal electrical pulse frequency and amplitude provide the best results, although very good results are produced over a wide range of parameters.

This paper has been devoted to presenting the newly discovered technique and understanding its underlying physical and chemical principles of operation. Clearly, more research, which is outside the scope of the current paper, is necessary before the technique may be successfully applied to real cases. In particular, the technique needs to be tested on various substrates, other than the metals used in this study, with aged fingerprints, etc. A thorough comparison of the technique to other known techniques for the development of sebaceous fingerprints is also in order. In particular, its use as a complementary method (e.g., with the cyanoacrylate method (1)) should be considered. However, one clear advantage of the technique is that the development is performed in a gaseous phase (12).

Acknowledgments

This research has been supported by the Division of Identification and Forensic Science, Israel Police Headquarters. We are grateful to Dr. Joseph Almog, Mr. Eliot Springer, and Dr. Arieh Frank for their continued interest and for many helpful discussions. All XPS measurements were conducted at the Tel-Aviv University Wolfson Applied Materials Research Centre by Dr. Larisa Burstein. We thank Professor Yoram Shapira, Director of the Center, and Dr. Larisa Burstein, for their help and for valuable discussions.

References

1. Margot P, Lennard C. Manual of fingerprint detection techniques, Universite de Lausanne, Lausanne, 1990.
2. Nasser E. Fundamentals of gaseous ionization and plasma electronics, Wiley-Interscience, New York, 1971.
3. Ben-Shalom A, Kaplan L, Boxman RL, Goldsmith S, Nathan M. SnO_2 transparent conductor films produced by filtered vacuum arc deposition, Thin Solid Films 1993 Dec;236:20–6.
4. Knowles AM. Aspects of physico-chemical methods for the detection of latent fingerprints, J Physics E 1978 Aug;11:713–21.
5. Halahmi E, Kronik L. Color Corona Discharge Images, IEEE Trans. Plasma Sci (special issue) 1996 Feb;24:87–8.
6. Briggs D, Seah M. Practical surface analysis, Second edition, John Wiley & Sons, NY, 1990.

7. Moulder JF, Stickle WF, Sobod PE. Handbook of X-ray photoelectron spectroscopy, Perkin-Elmer corporation, Minnesota, 1992.
8. Chang JS, Lawless PH, Yamamoto T. Corona discharge processes, IEEE trans Plasma Sci 1991 Dec;19:1152–65.
9. Razumovskii SD, Zaikov GE. Ozone and its reactions with organic compounds. Elsevier, New-York, 1984.
10. Kogelschatz U. Silent discharges and their applications, Proc. 10th International Conference on Gas Discharges and Their Applications, Swansea, 1992 Sep;2:972–80.
11. Horvath M, Bilitzky L, Huttner J. Ozone, Elsevier, Amsterdam, 1985.
12. Almog J, Gabay A. Chemical reagents for the development of latent fingerprints. III: Visualization of latent fingerprints by fluorescent reagents in vapor phase. J Forensic Sci 1980 Apr;25:408–10.

Additional information and reprint requests:
Erez Halahmi
Department of Interdisciplinary Studies
Faculty of Engineering
Tel-Aviv University, Ramat-Aviv 69978
Israel
E-mail:erez@eng.tau.ac.il